CHAPTER - 1

A Brief Overview of Computational Methodology

1. Introduction

This thesis revolves around the examination of the structural arrangements of certain psychedelic compounds, such as psilocybin, psilocin, and mescaline, as well as sulfur-containing molecules like dithiothreitol and thioglycolic acid. The investigation encompasses an exploration of intramolecular and intermolecular hydrogen bonding. Additionally, it aims to verify Surface-Enhanced Raman Spectroscopy (SERS) results through the use of simulated Raman spectra, with a particular focus on understanding interactions between molecules and metal clusters.

The subsequent sections will provide concise introductions to various aspects covered in this thesis, including conformational analysis, non-covalent interactions, sulfur-centered hydrogen bonding, and the computational techniques employed in this research.

1.1 Conformational Analysis

Molecules display a variety of shapes and functionalities contingent upon their chemical surroundings. These unique spatial configurations arising from rotations around individual bonds are referred to as conformers or conformational isomers.[1] In cases of conformational isomerism, it is often observed that molecules tend to favor one particular geometry over another in a given physical condition. This preference is primarily influenced by interactions among different components of the molecule or by the presence of surrounding environment, including solvent moieties. These interactions, whether attractive or repulsive, play an essential part in establishing the stability of conformers.[2]

Interactions occurring within the same molecule are denoted as intramolecular interactions, while those occurring between two different binding partners are known as intermolecular interactions. Conformational analysis involves conducting a thorough examination of the potential energy manifolds of a molecule in order to assess the various

molecule's conformers. It also includes evaluating their energies and understanding the electronic effects that dictate their stability.

Exploration of the conformational space of a molecule commenced during the mid-20th century, thanks to the groundbreaking contributions of Barton and Hassel. In recognition of their remarkable contributions to the comprehension and application of conformational concepts in chemistry field, they were jointly awarded the Nobel Prize in 1969.[3] In particular, Barton's 1950 publication titled "The conformation of the steroid nucleus"[4] drew upon earlier studies by Hassel [5,6] on electron diffraction of cyclohexane derivatives. Through this work, Barton demonstrated that biologically active steroid molecules adopt specific conformations, which significantly influence their chemical and physical properties. This revelation led to the realization that molecular geometries have a vital role in shaping the configuration, reactivity, and spectroscopic behavior of molecules. As a result, a comprehensive understanding of molecular structures became indispensable across diverse scientific disciplines, encompassing spectroscopy, organic synthesis, materials design, and biochemistry, to name a few.[2,7–9]

Conformation analysis experienced a significant boost with the advancement of sophisticated spectroscopic techniques and the increased capabilities of computational chemistry.[7] As a result, it has become a crucial tool for investigating complex reactions in metal-catalysis, organo-catalysis, and the development of new catalysts.[8–11] The elucidation of conformers through frequency domain spectroscopy has been a well-utilized approach. Various experimental techniques for instance UV,[12] NMR,[2] X-ray,[13] electron diffraction,[14] infrared,[15] Raman,[16] microwave spectra,[17] photoelectron spectroscopy,[18] supersonic molecular jet spectroscopy,[19] optical rotatory dispersion (ORD),[20] and Circular dichroism (CD)[21] measurements have been extensively employed in conformational studies. Furthermore, the emergence of femtosecond pulsed lasers has facilitated the seamless unraveling of conformational analysis and associated dynamics.[22–25]

In addition to experimental methods, computational tools have proved to be a powerful means of studying molecular conformations.[26] The joint recipients of the 1998 Nobel Prize in Chemistry were Walter Kohn and John A. Pople. Walter Kohn's recognition stemmed from his instrumental role in shaping the density-functional theory, whereas John A. Pople's accolade celebrated his pioneering contributions to computational techniques in the realm of quantum chemistry. Pople's innovative concepts paved the way for the creation of software used for forecasting and comprehending molecular structures along with their properties.[27] Numerous factors contribute to determining the conformation of a molecule, with non-covalent interactions playing a particularly significant role in dictating its specific arrangement. The upcoming section will provide a concise introduction to non-covalent interactions, which are instrumental in stabilizing molecules.

1.2 Non-covalent interactions

Non-covalent interactions (NC-interactions) are omnipresent in various states of matter and they define the 3D crystal structure of organic and organometallic components. These interactions are crucial in influencing the stability of molecules and molecular clusters, as well as influencing the functionality of biomolecules and materials. In fact, they are fundamental to numerous biological processes and are considered the cornerstone of life processes.[28–35] Additionally, NC-interactions have a profound impact on the properties of supramolecular species, significantly shaping their characteristics.

1.2.1 Types of non-covalent interactions/H-bonding interactions

Non-covalent interactions (NCI) are commonly classified into three distinct categories[28]:

(a) Very Strong NC-interactions (15-40 kcal/mol)

(b) Strong NC-interactions (4-15 kcal/mol)

(c) Weak NC-interactions (< 4 kcal/mol)

which help to distinguish the relative strengths of various forms of NC-interactions. This classification is rooted in the concept of complex energy or stabilization energy, extensively explored by Desiraju and Steiner in their book.[28] When the donor and acceptor atoms engage actively in bonding, either within a single molecule or between separate molecules, it results in the formation of highly robust NC- bonds. The change from an exceedingly potent NC- bond to a strong NC- bond signifies a shift from a quasi-covalent nature to a more electrostatic nature of the bond. On the other hand, weak NC-bonds are also electrostatic in nature, with dispersive and charge transfer contributions being the dominant components. Nonetheless, these weak NC-bonds are still stronger than van der Waals interactions.[28]

1.2.2 H-bonding

The concept of H-bonding has a rich history, with the first report dating back to 1920 by Latimer and Rodebush.[36] Hydrogen bonds belong to the class of non-covalent interactions and have been extensively studied over the years. Similar to other chemical bonds, hydrogen bonds exhibit directional behavior. This unique characteristic allows them to play a significant role in conformational arrangements and molecular associations.[28] One of the seminal works in the field of H-bonding was conducted by Linus Pauling.[37] His research provided a rationale for the existence of H-bonding.[38] According to this perspective, hydrogen bonds are formed by the electrostatic attraction between two atoms, typically with high electronegativity, implying a predominantly ionic nature. Pauling focused on the presence of conventional H-bonds. In 1960,[39] Pimentel and McClellan expanded the understanding of hydrogen bonding. According to their definition, the criteria that follow must be satisfied for a H-bond to form between a functional group A-H and an atom or group of atoms B, whether they are within the same molecule or distinct molecules:

(a) The presence of bond formation is supported by evidence of association or chelation.

(b) The hydrogen atom that is already connected to A is a part of the connection that connects A-H and B.

Notably, the H-bonding definition intended by Pimentel and McClellan did not rely on the concept of electronegativity and charge polarization.[39] A more recent and updated definition of H-bonding was established in 2011 by the IUPAC committee,[40] which defines a H-bond as an attractive linkage between an atom or group of atoms within the same or different molecules and a hydrogen atom originating from a molecule or molecular fragment X-H, where X holds greater electronegativity than H. H-bonding serves as a fundamental pillar in living organisms as it has a vital impact in the assembly of amino acid monomers, facilitating the formation of proteins and enzymes.[41] The hydrogen bonds are classified into two categories, namely conventional/classical and unconventional/Non-classical hydrogen bonds, based on the donor-acceptor atoms involved in the interactions.

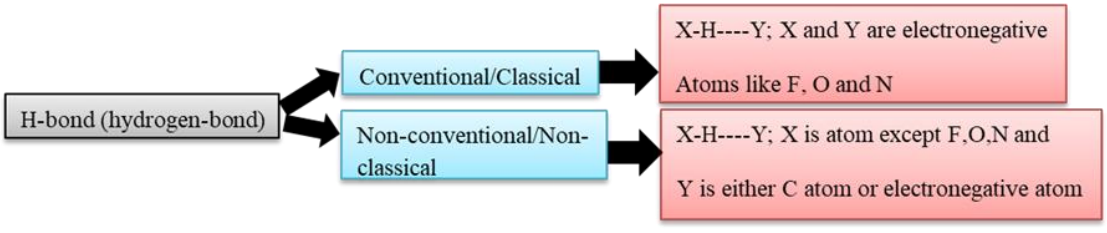

Figure 1.1: Schematic representation of different types of H-bonding

The above schematic figure illustrates the interaction, where X functions as a proton donor and Y as a proton acceptor. H-bonding is a donor-acceptor orbital interaction, with Y donating its electron pair into the adjacent X-H bond's antibonding orbital. The potency of the H-bonding interaction relies on variables such as the electronegativity of X and Y atoms, directionality, orbital overlap, and the energies of the donor and acceptor orbitals. In classical or conventional H-bonding, X and Y atoms are typically electronegative atoms like F, O, and N. These interactions have bond energies ranging from 20 to 50 kcal/mol.[28,42,43] On the other hand, unconventional or non-classical hydrogen bonding occurs when X or Y, or both, are less electronegative atoms. Examples include S-H----S, C-H----S, O-H----S, etc., with bond energies ranging from 1-20

kcal/mol.[42,43] While conventional hydrogen bonding has been extensively studied, unconventional hydrogen bonding is relatively less explored. It is important to note that in any form of hydrogen bonding, there is a partial transfer of a proton to the donor moiety. If a complete transfer occurs, it would be considered an acid-base reaction.

1.2.3 Sulfur centered H-bonding(SCHBs)[Unconventional/non-classical]

While hydrogen bonds involving oxygen and nitrogen atoms have received extensive research attention, sulfur-containing hydrogen bonds have often been overlooked due to their perceived weaker and more dispersive nature, primarily attributed to the lower electronegativity of sulfur (2.6). Sulfur-centered H- bonds (SCHBs) are a type of unconventional hydrogen bond (UHB), similar to the conventional H- bond (CHB). Similar to (CHBs), (SCHBs) exert a significant influence on the crystal structure, interactions between solvents and solutes, and the overall stability of molecular systems.[44,45]

In the early reports on hydrogen bonds, SCHBs (sulfur-centered hydrogen bonds) were not recognized as valid hydrogen bonds. Nevertheless, Gordy et al. confirmed the formation of hydrogen bond in molecules containing sulfur such as pyridine, dibenzylamine, and α-picoline, shedding further light on their existence and significance.[46] The report by Gordy et al. paved the way for further exploration of SCHBs. Following that, numerous studies were undertaken to validate the participation of sulfur atoms in hydrogen bonding.[28,47,48] In 1981, Hoyer was the first to observe intramolecular hydrogen bonding in N-acyl-thioureas.[49] The biological activity of methionine and tyrosine elucidated by Biswal et al. through experiments supported the significance of SCHBs. They employed model compounds such as phenol, p-cresol, dimethyl sulfide, and 2-napthol, and conducted experiments using laser-induced fluorescence in a supersonic jet spectroscopic technique.[44] In 2009, Biswal et al. published another significant report on SCHBs, focusing on the study of complexes between H_2S and indole, as well as 3-methyl indole. Their study conclusively attributed the stability of these modeled complexes to the S-H---π interactions.[50] Numerous

investigations, employing both experimental and computational approaches, were conducted to elucidate the characteristics, strength, and directionalities of SCHBs.

In addition to SCHBs, NC-interactions such as C–H----Y and X–H----π have also demonstrated their significance.[51] Despite being weaker, the C–H----O interaction, for instance, has been shown to have important role in stabilizing molecular complexes, particularly those with cyclic structures and various other systems.[51,52] In contrast, π-bonds possess an abundance of electrons and can serve as hydrogen bond acceptors, substituting for electronegative atoms like F, O, and N. A notable illustration of this is the benzene-water complex, which forms an O–H...π hydrogen bond.[53]

1.3 Molecule-metal cluster Interaction

Studying catalyses theoretically poses challenges mainly due to the fact that the reactions involved take place solely on an infinite surface in the experiment. This necessitates finding a middle ground between cluster physics and solid-state. Building upon the early studies conducted by Upton et al.[54,55] and Bauschlicher et al.,[56] a prevalent method involves using small clusters of metal as exemplar models for the boundless surface of metal. This approach has garnered significant interest and has been extensively employed in various theoretical investigations emphasizing the adsorption of atoms and molecules on metal systems. Gold, a coinage metal, is renowned for its inert nature in bulk form. However, it has been discovered that gold exhibits activity in its cluster forms which are smaller than 3-4 nm in size. Small molecules' adsorption characteristics, such as O2, N2, H2, CO, and NO, onto gold clusters, is significantly influenced by the size and charge states of the Au clusters.[57–61] The enhanced catalytic activities observed in clusters with confined sizes are not exclusive to gold (Au) clusters; they also apply to other clusters of coinage metal. As an example, clusters of silver (Ag) and copper (Cu) display catalytic capabilities akin to those of clusters of Au in processes like the low-temperature CO oxidation and hydrocarbons's partial oxidation. This implies that the remarkable catalytic efficiency of small size clusters extends to other clusters of coinage metals like Ag and Cu. [45,46] Ag and Cu-based nano-catalysts's catalytic processes can therefore be better

understood by examining the Ag and Cu clusters's adsorption behavior.

The use of DFT methods has been widely recognized in the literature as an effective approach for predicting the interactions between adsorbed molecules or moieties and metal surfaces. Several studies have demonstrated the efficiency of DFT in this regard.[62–65] Notably, T.D. Hieu et al. employed DFT to investigate the SERS of the thiram pesticide on copper clusters, and their computational predictions strongly supported the corresponding experimental results.[66] Moreover, previous research by Ahmed et al. highlighted the suitability of small-sized copper clusters as efficient models for representing the metal surface in adsorption studies.[67] Literature has unveiled that these model surface clusters offer the best extrapolation to the metal surface's properties.[68] Hence, in this thesis, the DFT method was employed to gain comprehensive understanding of the binding/interacting modes between molecules and metal clusters.

1.4 Computational Methods

The electronic structures of molecules, which provide insights into their molecular properties, can be ascertained by resolving the Schrödinger wave equation for systems with multiple electrons. This fundamental equation forms the basis of quantum chemical calculations, enabling access to various molecular properties. A variety of quantum chemical methods are employed to study molecular systems, including semi-empirical methods (such as AM1 and PM6), ab initio methods as HF, MP2, CCSD, and CCSD(T), and DFT methods for instance BLYP, B3LYP, and M06. Among these methods, ab initio and DFT are widely preferred and commonly utilized for elucidating modeled molecular systems.[69]

1.4.1 Born-Oppenheimer approximation

The Born-Oppenheimer approximation was formulated in 1927 through the collaborative efforts of Max Born and J. Robert Oppenheimer. This fundamental concept serves as a valuable tool for simplifying the complexity of quantum chemical calculations when assigning quantum states of molecules. By assuming the separation of nuclear and electronic motions, the Born-Oppenheimer approximation allows for a more tractable

analysis of molecular systems and facilitates the study of their quantum behavior. According to the Born-Oppenheimer approximation, atomic nuclei move much more slowly and nearly stationary than do electrons inside a molecular system. This approximation is based on the significant difference in mass between the nuclei and electrons, allowing for a simplified treatment of the electronic structure while treating the nuclear positions as fixed. As a result, the time independent Hamiltonian (for a system with multiple electrons and two nuclei) is formulated without including the nuclei's kinetic energy. The Hamiltonian can be expressed as:

$$\hat{H}(r, R) = 1/2 \sum_i \nabla_i^2 - (\sum_i \sum_I (Z_I/|R_I - r_i|) + \sum_i \sum_{j<i} (1/|r_i - r_j|) + \sum_i \sum_{J<I} (Z_I Z_J/|R_I - R_J|)) \quad (1)$$

In the given expression, ∇ denotes the Laplacian operator, Z_I and Z_J represents the atomic numbers of atoms 'I' and 'J' respectively. While R_I and R_J corresponds to the coordinates of nuclei I and J. whereas, r_i represents the positions of electrons. In the provided equation the initial term denotes the electrons's kinetic energy, while the second term accounts for the mutual repulsion between the electrons as well as their attraction to the nuclei.[70]

1.4.2 Density functional theory

Currently, Density Functional Theory stands out as highly effective and remarkable approach for studying many-body systems. The foundational underpinning of this theory can be linked to the groundbreaking research of Thomas and Fermi,[71,72] which was later expanded upon by Thomas-Fermi-Dirac.[73–75] However, it was the groundbreaking contributions of P. Hohenberg and W. Kohn in 1964,[76] followed by W. Kohn and L. J. Sham's influential work in 1965,[77] that truly revolutionized the field.

1.4.2.1 Hohenberg-Kohn Theorems

Theorem 1: The total energy and the external potential $V_{ext}(r)$ can be uniquely described as functionals of the electron density [n(r)]. In other words, the electron density [n(r)] governs both the precise number of electrons and the modeled system's total energy, denoted as E[n(r)].

Hence, E[n(r)], the energy functional can be formulated in terms of both the external potential $V_{ext}(r)$ and the electron density [n(r)] in the subsequent manner:

$$E[n(r)] = \int n(r)V_{ext}(r)dr + F[n(r)] \qquad (2)$$

Here, F[n(r)] represents a universal functional that depends solely on [n(r)], the electron density.

The Hamiltonian of the system, associated with the energy functional, can be expressed in a way that its expectation value provides the ground state energy, as follows:

$$E[n(r)]=<\psi\hat{H}\psi> \qquad (3)$$

The Hamiltonian can be represented as: $\hat{H} = F + V_{ext}$

Here, $F = T + V_{ee}$; $V_{ee} = J$ + nonclassical term

The potential energy arising from electron repulsion, V_{ee}, is composed of a classical repulsion term J and a non-classical exchange-correlation term. F, the electron operator is uniform for all N electrons, thus defining the Hamiltonian operator $\hat{H}$ in terms of N and the external potential V_{ext} (r).

Theorem 2: The ground state energy can be ascertained through variational determination, implying that the density minimizing the total energy aligns with the precise ground state, i.e.

$$E_0 \leq E[n(r)] \qquad (4)$$

Here, E[n(r)] represents the energy functional, which bears resemblance to the variational principle of the wave function i.e. $E_0 \leq E(\psi')$.

1.4.2.2 Kohn-Sham Equation

Kohn-Sham introduced an alternative approach to handle many-body interacting systems by employing an auxiliary non-interacting one-body system.[77] This equation is derived

from the fundamental assumption that the electron density of an interacting system's ground state can be approximated by the electron density of a non-interacting system, with an effective potential V_{eff}. Therefore, the Kohn-Sham Hamiltonian can be expressed as follows:

$$H_{KS} = -\frac{1}{2}\nabla^2 + V_{eff} \qquad (5)$$

The expression for the kinetic energy of the non-interacting system of interest is given by:

$$T[\rho] = \sum_i^N \langle \psi_i \left| -\frac{1}{2}\nabla_i^2 \right| \psi_i \rangle \qquad (6)$$

The above equation demonstrates that the kinetic energy is reliant on non-interacting system's electron density, and it can be expressed as:

$$\rho(r) = \sum_i^N \sum_{r,s} |\psi_i(r,s)|^2 \qquad (7)$$

These are Schrödinger equation solutions for N non-interacting electrons moving in Kohn-Sham effective potential, $V_{eff}(r)$, defined by:

$$V_{eff}(r) = V(r) + \frac{\delta J[\rho]}{\delta \rho(r)} + \frac{\delta E_{XC}[\rho]}{\delta \rho(r)} \qquad (8)$$

$$= V(r) + \int \frac{\rho(r')}{|r-r'|}\, dr' + V_{XC}(r) \qquad (9)$$

where $V_{xc}(r)$ represents the exchange-correlation potential,

$$V_{XC}(r) = \frac{\delta E_{XC}[\rho]}{\delta \rho(r)} \qquad (10)$$

Therefore, through the solution of N one-electron Schrödinger equation, the electron density can be determined for a given $V_{eff}(r)$,

$$\left[-\frac{1}{2}\nabla^2 + V_{eff}(r)\right]\psi_i = \varepsilon_i \psi_i \qquad (11)$$

Equations (1.9-1.11) form the Kohn-sham equations. Till self-consistency is reached, these equations are solved recursively. The total energy can be calculated using the following equation:

$$E = \sum_i^N \varepsilon_i - \frac{1}{2}\int \frac{\rho(r)\rho(r')}{|r-r'|} dr dr' + E_{XC}[\rho] - \int V_{XC}(r)\rho(r) dr \qquad (12)$$

Similarly, both the Hartree-Fock equation and the Kohn-Sham equation offer a one-body equation for describing many-body systems. However, from a fundamental perspective, the Kohn-Sham approach differs significantly from the Hartree-Fock theory as it incorporates the influence of exchange-correlation effects on electrons in a more comprehensive manner. In the Kohn-Sham method, the exact formulation of the exchange and correlation functional was not achieved. Consequently, several approximate methods were developed to address the exchange-correlation functional in practical calculations.

1.4.2.3 Exchange-Correlation Energy

The exchange-correlation functional, E_{XC} *[ρ]*, in the Kohn-Sham equation is of utmost importance in obtaining more accurate results. It can be divided into two contributions: the exchange term, E_X [ρ], and the correlation term, E_C [ρ].

$$E_{XC}[\rho] = E_X[\rho] + E_C[\rho] \qquad (13)$$

In DFT, exchange-correlation approximations are classified into three primary categories: the Local Density Approximation (LDA), the Generalized Gradient Approximation (GGA), and Hybrid Functional. In the LDA approach, the approximate exchange-correlation functional depends solely on the local electron density. Some examples of LDA methods are SVWN,[78] and PVWN5[78] . On the other hand, in GGA-based (Generalized Gradient Approximation) methods, the gradient of the electron density is also considered along with the local electron density to define the approximate exchange-correlation functional. Some examples of the GGA method include BLYP[79,80], PW91[81], and B88[82]. In hybrid DFT functionals, a fraction of the Hartree-Fock method is incorporated into the exchange energy component along with the DFT method. This Hartree-Fock exchange mixing provides an easy way to improve a variety of molecular properties, including atomization energies, structural parameters, and vibrational frequencies, which may be inadequately described by standard exchange-correlation

functionals. Some examples of Hybrid DFT methods include B3LYP[79,80] and M06-2X.[69,83]

1.4.3 Møller-Plesset perturbation theory

Perturbation theory has been widely used in quantum chemistry to assess the atomic and molecular electronic structure. In 1934, Møller and Plesset[84] pioneered second-order perturbation theory as an extension to the Hartree-Fock (HF) method, enabling the acquisition of the system's corrected electron pair correlation energy. Within Møller-Plesset perturbation theory, the Hartree-Fock approach is augmented with elevated excitations, serving as a non-iterative correction. This approach quantitatively improves the accuracy of the Hartree-Fock method. The foundation of perturbation theory lies in the partitioning of the Hamiltonian into two distinct components:

$$H = H^{(0)} + \lambda V \qquad (14)$$

Where $H^{(0)}$ represents the zeroth-order Hamiltonian and λV represents the perturbation applied to $H^{(0)}$ (with the applied correction being small compared to $H^{(0)}$). The zeroth-order Hamiltonian $H^{(0)}$ is defined as the sum of the Fock operators, as shown below:

$$\hat{\mathrm{H}}^{(0)} = \sum_p \hat{\mathrm{F}}(p) = \sum_p \hat{\mathrm{h}}(p) + \sum_{p,i}[\hat{\mathrm{J}}_i(p) - \hat{\mathrm{K}}_i(p)] \qquad (15)$$

The operator $\hat{\mathrm{h}}(p)$ represents the one-electron operator related to the kinetic energy and the attraction between the nucleus and electron p. Additionally, $\hat{\mathrm{J}}_i(p)$, and $\hat{\mathrm{K}}_i(p)$ correspond to the Coulomb and exchange operators, respectively, which constitute the Hartree-Fock potential. These operators are represented using spin orbitals ψ_i:

$$\hat{\mathrm{J}}_\mathrm{i}(1)\psi_\mathrm{j}(1) = [\int \mathrm{dr}_2 \psi_\mathrm{i}^*(2)\frac{1}{\mathrm{r}_{12}}\psi_\mathrm{i}(2)]\psi_\mathrm{j}(1) \qquad (16)$$

$$\hat{\mathrm{K}}_\mathrm{i}(1)\psi_\mathrm{j}(1) = [\int \mathrm{dr}_2 \psi_\mathrm{i}^*(2)\frac{1}{\mathrm{r}_{12}}\psi_\mathrm{j}(2)]\psi_\mathrm{i}(1) \qquad (17)$$

(here, 1 and 2 represent the positions r_1 and r_2 of electrons 1 and 2, respectively.)

Assuming that V is a small perturbation to H_0, it is reasonable to express the perturbed wavefunction and energy as a power series in V. This can be achieved by introducing the parameter λ in the following manner:

$$\psi = \psi^{(0)} + \lambda\psi^{(1)} + \lambda^2\psi^{(2)} + \lambda^3\psi^{(3)} + \cdots \qquad (18)$$

$$E = E^{(0)} + \lambda E^{(1)} + \lambda^2 E^{(2)} + \lambda^3 E^{(3)} + \cdots \qquad (19)$$

The Schrödinger equation is then modified using the perturbed wavefunction and energy obtained from the power series expansion as follows:

$$H^{(0)} + \lambda V\left(\psi^{(0)} + \lambda\psi^{(1)} + \cdots\right) = (E^{(0)} + \lambda E^{(1)} + + \cdots)(\psi^{(0)} + \lambda\psi^{(1)} + \cdots) \quad (20)$$

The HF wavefunction $\varphi^{(0)} = \varphi^{HF}$ is considered as the zeroth-order wavefunction. The relevant eigenvalue is derived by adding up the energies of the orbitals:

$$E^{(0)} = E^{orb} = \sum_i^{occ} \varepsilon_i \qquad (21)$$

Therefore, the Hartree-Fock wavefunction encompasses the designated model space P, while the Q-space is constituted by the substitution functions φ_s, that are generated through excitations of electrons from occupied spin orbitals ψ_i, ψ_j, ... to virtual orbitals ψ_a, ψ_b, ... (where ψ_p, ψ_q, ... represent general spin-orbitals). These excitations include single (S), double (D), triple (T), and so on. The functions φ_s, such as φ_i^a, φ_{ij}^{ab}, φ_{ijk}^{abc}, and so on, are orthogonal to φ^{HF}, which greatly simplifies the calculation of various energy corrections. In Møller-Plesset theory the perturbation operator is expressed as:

$$\hat{V} = \hat{H} - \hat{H}^{(0)} = \sum_{p\geq q} \frac{1}{r_{pq}} - \sum_{p,i}[\hat{J}_i(p) - \hat{K}_i(p)] \qquad (22)$$

The first-order correction energy, denoted as $E^{(0)}$, is obtained by applying the perturbation operator as follows:

$$E_{MP}^1 = <\varphi^{(0)}|\hat{V}|\varphi^{(0)}> = V_{00} = -\frac{1}{2}\sum_{ij} <ij||ij> \qquad (23)$$

Where the double bar integral represents an anti-symmetrized two-electron integral of a general form:

$$<pq||rs> = \iint \psi_p^*(1)\psi_q^*(2)\frac{1}{r_{12}}[\psi_r(1)\psi_s(2) - \psi_s(1)\psi_r(2)]d\tau_1 d\tau_2 \qquad (24)$$

Where τ represents the integration over the spatial and spin coordinates of the spin orbitals ψ.

Therefore, the HF energy equates to the MP1 energy

$$E(HF) = E(MP1) = \sum_i^{occ} \varepsilon_i - \frac{1}{2}\sum_{ij}^{occ} <ij||ij> \qquad (25)$$

In other words, the HF method maintains accuracy up to the first-order of Møller-Plesset perturbation theory (MPPT), as initially established by Møller and Plesset. This inclusively applies to electron density, dipole moment, and various one-electron properties, and is known as the Møller-Plesset theorem.

The following equation expresses the MP2 correlation energy correction:

$$E_{MP}^{(2)} = \sum_{s>0} \frac{V_{0S} - V_{S0}}{E_0 - E_S} \qquad (26)$$

In this equation, the S substitutions ($\varphi = \varphi_i^a$) do not contribute due to the Brillouin theorem, which implies that $< \varphi^{(0)} \left| \widehat{\mathrm{V}} \right| \varphi_i^a > = 0$. Only D excitations ($\varphi_s = \varphi_{ij}^{ab}$) contribute to the finite matrix elements V_{0s}, as T, Q, etc. excitations are excluded due to the Slater–Condon rules.[85,86]

Following the application of Slater–Condon rules, the second-order correction can be formulated in the following manner:

$$E_{MP}^{(2)} = \frac{1}{4} \sum_{ij}^{occ} \sum_{ab}^{vir} < ij||ab > a_{ij}^{ab} \qquad (27)$$

accompanied by

$$a_{ij}^{ab} = (\epsilon_i + \epsilon_j - \epsilon_a - \epsilon_b)^{-1} < ab||ij > \qquad (28)$$

As the magnitudes of the D excitations.

1.4.4 Coupled cluster (CC) methods

Coupled cluster is a computational method employed to characterize many-body systems. Although it also has uses in nuclear physics, it is frequently used as one of numerous post-Hartree-Fock ab initio approaches in the field of computational chemistry. Coupled cluster builds upon the fundamental HF molecular orbital approach by incorporating the exponential cluster operator to capture electron correlation. This technique is highly regarded for its accuracy and is often employed for precise calculations of small to medium-sized molecules. The technique was first formulated by Fritz Coester [87] and Hermann Kümmel[63] in the 1950s for investigating phenomena in nuclear physics. When Jiří Čížek,[88] and later in collaboration with Josef Paldus,[89] improved the technique in 1966 to address electron correlation in atoms and molecules, its use became more widely used. It is currently one of the most popular methods for including electronic correlation

in quantum chemistry. The Many Electron Theory (MET), put forth by Oktay Sinanoğlu, and providing a precise and variational solution to the many-electron problem, can be thought of as the perturbative form of CC theory. Additionally, it was known as "Coupled Pair MET (CPMET)". As a result, the CC method is both simpler and more accurate in terms of computational calculations. Consequently, the CC method represents the most refined form of MET, yielding highly precise results that closely align with experimental observations.[90]

A precise response to the time-independent Schrödinger equation is provided by coupled-cluster theory

$$H|\Psi> = E|\Psi> \qquad (29)$$

The wavefunction in coupled-cluster theory is expressed using an exponential ansatz:

$$|\Psi> = e^{T}|\Phi> \qquad (30)$$

The reference wave function in this formulation is denoted by |Φ>. It is frequently a Slater determinant obtained from HF molecular orbitals. However, various wave functions can also be used, such as multi-configurational self-consistent field, Brueckner orbitals, and configuration interaction. When the cluster operator T acts on the variable |Φ>, it generates a linear combination of excited determinants that stem from the reference wave function.

In the following form the cluster operator can be shown as:

$$T = T_1 + T_2 + T_3 + \ldots \qquad (31)$$

where T1 stands for the operator for every single excitation, T2 for every double excitation, and so on. According to the second quantization formalism, these excitation operators are represented as:

$$T_1 = \sum_i \sum_a t_a^i \hat{\alpha}^a \hat{\alpha}_i \qquad (32)$$

$$T_2 = \frac{1}{4}\sum_{i,j} \sum_{a,b} t_{ab}^{ij} \hat{\alpha}^a \hat{\alpha}^b \hat{\alpha}_j \hat{\alpha}_i \qquad (33)$$

and for the cluster operator of general n-fold excitations

$$T_n = \frac{1}{(n!)^2}\sum_{i_1,i_2,i_3 \ldots\ldots i_n} \sum_{a_1,a_2,\ldots\ldots,a_n} t_{a_1,a_2,\ldots\ldots,a_n}^{i_1,i_2,i_3 \ldots\ldots i_n} \hat{\alpha}^{a_1}\hat{\alpha}^{a_2} \ldots\ldots \hat{\alpha}^{a_n}\hat{\alpha}_{i_n} \ldots \hat{\alpha}_{i_2}\hat{\alpha}_{i_1} \qquad (34)$$

When we consider only the cluster operators T_1 and T_2 of T, we can expand this exponential operator e^T as a Taylor series as follows:

$$e^T = 1 + T + \frac{1}{2!}T^2 + \cdots = 1 + T_1 + T_2 + \frac{1}{2}T_1^2 + T_1T_2 + \frac{1}{2}T_2^2 + \cdots \quad (35)$$

The following types of coupled-cluster methods:

Based on the maximum number of allowable excitations in the cluster operator T, traditional coupled-cluster approaches are categorized. Commonly, these procedures are denoted by abbreviations that begin with "CC" (for coupled cluster), then:

S denotes single excitations, often known as "singles" in coupled-cluster jargon.

D represents double excitations, sometimes known as "doubles"

T denotes triple excitations, sometimes known as "triples"

Q denotes quadruple excitations, often known as "quadruples"

These abbreviations indicate the level of electron excitations considered in the coupled-cluster calculations.

The intricacy of equations and the associated computer codes, as well as the computational expense, significantly escalate as the level of excitation increases. In numerous applications, CCSD, despite being relatively affordable, lacks the required accuracy, except for the smallest systems with approximately 2 to 4 electrons. In such cases, an approximate treatment of triples is often necessary. CCSD(T) is the most renowned coupled-cluster method, known for providing an estimate of connected triples. It offers a reliable description of closed-shell molecules, particularly in the vicinity of their equilibrium geometry. CCSD (single and double excitations) is a convenient approach, but the inclusion of disconnected triples (CCSDT) significantly increases the computational cost. The CCSD(T) method, which gives a perturbative estimate of the impact of triple excitations, is frequently denoted as the benchmark/gold standard in computational chemistry.[69,91]

1.4.5 Basis set

The electronic properties of molecular systems are represented by the molecular orbitals, which are created using mathematical functions.[69] Molecular orbitals (ψ_i) are formed through linear combinations of n basis functions (φ_μ)

$$\psi_i = \sum_{\mu=1}^{n} C_{\mu i}\varphi_\mu \qquad (36)$$

Here, $C_{\mu i}$ represents the coefficients or expansion coefficients of the molecular orbitals, also referred to as the molecular orbital coefficients.

In general, basis functions are centered on individual atoms and are commonly referred to as atomic basis functions. Both the type of the employed basis functions and the size of the basis sets influence the precision of the outcomes. In a general sense, a basis set comprises a set of functions, usually resembling atomic orbitals, employed to build molecular orbitals via a linear combination of atomic orbitals (LCAO). Therefore, the adequacy of theoretical and computational calculations relies on selecting the appropriate basis set.[69] For theoretical and computational calculations, a finite set of basis functions is used. In the realm of quantum chemical calculations, a range of basis sets have been created, with the minimal basis set and split-valence basis set standing out as two of the most extensively utilized options.

Minimal basis sets comprise a constrained count of basis functions, which prove adequate for depicting the electronic structure of the molecular system across all electrons. However, they lack flexibility in fully representing the electron distribution within atomic orbitals, particularly when dealing with non-spherical electron distributions in the orbitals. To address the limitations of minimal basis sets, split-valence basis sets were formulated, which involve doubling all the basis functions. This allows for a more flexible and accurate representation of the electron distribution in atomic orbitals. The split-valence basis set is formed by combining double basis sets, consisting of inner and valence sets, along with the linear combination of similar orbitals with different effective charges.[92] This approach involves multiple basis functions for each

valence atomic orbital, including double, triple, or quadruple-zeta type bases, to provide a more comprehensive representation.[69]

1.4.6 Complete basis set (CBS) limit extrapolation

Complete basis set accuracy offers computational chemists an alternative route to obtain more reliable approximate results of infinitely larger basis sets. This is achieved by utilizing the results obtained from finite larger basis sets, without incurring any additional computational cost. CBS accuracy provides a valuable approach for achieving higher levels of precision in quantum chemical calculations. Overall, the CBS limit holds special significance for post-Hartree-Fock methods that encompass the incorporation of electron correlations. These calculations are computationally demanding. The Helgaker method is commonly employed to extrapolate the correlation energy using cc-pVNZ [93] basis sets, where N represents the level of basis set (such as T for triple-zeta and Q for quadruple-zeta)[94]:

$$E_{Corr} = a + bX^{-3} \qquad (37)$$

Here, E_{Corr} is correlation energy, X denotes the cardinal number, for instance, four in the case of quadruple-zeta sets or three for triple-zeta sets, and so forth.

1.4.7 Computation of Interaction Energy (IE)

To compute the interaction energy of a molecular cluster, we employ the subsequent equation:

$$\Delta E_{int}(AB) = E_{AB}^{AB}(AB) - E_{A}^{A}(A) - E_{B}^{B}(B) \qquad (38)$$

In the given equation, A and B represent the individual monomers, and AB denotes the molecular cluster. $E_{AB}^{AB}(AB)$ denotes the energy of the molecular cluster computed at a specific theoretical level. Similarly, $E_{A}^{A}(A)$ and $E_{B}^{B}(B)$ correspond to the monomers A and B's energies, respectively, computed at the same theoretical level employed for the energy calculation of molecular cluster.[95] In the current thesis work, the same equation was utilized to calculate the interaction energy of dimers containing different monomers or the same monomers.

1.4.7.1 Basis set superposition error (BSSE) Correction

During the process of cluster formation i.e. dimers, trimers and so on, the monomers come closer to each other, and during this process, they partially utilize each other's basis functions, resulting in additional stabilization within the overall cluster. This extra stabilization is termed "basis set superposition," and it is corrected using the following equation[96,97]:

$$\Delta E_{Int}^{CP}(AB) = E_{AB}^{AB}(AB) - E_{A}^{AB}(A) - E_{B}^{AB}(B) \qquad (39)$$

where, $\Delta E_{Int}^{CP}(AB)$ represents the counterpoise (CP) corrected interaction energy of the molecular cluster. $E_{A}^{AB}(A)$ denotes the monomer A's energy and $E_{B}^{AB}(B)$ denotes the monomer B's energy, AB for the A and B monomers refer to the full dimer basis set respectively, calculated at the same theoretical level as that employed for the calculation of the molecular cluster.

1.5 Computational tools

All computations in this thesis were conducted using the Gaussian16 software suite. The Gaussview interface of the Gaussian 16 software package[98] was utilized for all data visualization and job submission. The MultiWFN software[99] and VMD software[100] were used for performing AIM and NCI calculations using the wave functions generated by Gaussian16. The LED (local energy decomposition) calculation was performed using the ORCA 4.2 software[101]. All Gaussian calculations were conducted on the institute server, PARAM SHIVAY supercomputer at IIT (BHU), Varanasi.

1.6 Molecular Properties

1.6.1 Optimization of Geometry

The primary stage in quantum chemical computation involves optimizing the geometry of the molecule. In the majority of calculations, the gas phase is typically employed for studying isolated molecular systems. The purpose of performing geometry optimization is to assess the molecular structure with the lowest energy. A geometry optimization

involves adjusting the atomic positions within a molecule until the energy reaches its minimum value. This corresponds to the point of lowest energy on the potential energy surface. The geometry that has been optimized is often used for comparing with experimental data.

1.6.1.1 Dihedral relaxed scan

The exploration of the potential energy surface associated with dihedral angles involves incrementally varying the dihedral angle in small incremental steps to 360° thereby realise a complete rotation around the bond at an appropriate level of theory. Utilizing Internal Redundant coordinates (via the Opt=ModRedundant option) which conducts a geometry optimization at each step while keeping the scanned variable (in this case the chosen dihedral angle) constant. This process is commonly known as relaxed scan and the resultant surface is called Relaxed Potential Energy Surface (PES).

1.6.2 Analysis of vibrational modes

Vibrational mode analysis is essential to ensure that the optimized geometry is free from imaginary frequencies during the optimization process. Presence of an imaginary frequency indicates incomplete optimization that requires further refinement until the imaginary frequency is eliminated. Additionally, vibrational analysis provides a comprehensive molecular fingerprint, enabling precise molecular identification. Vibrational frequency computation approaches can offer a direct assessment of the strength of an H-bond interaction. The formation of a complex system commonly results in modifications to its structure, which are conjoined with alterations in vibrational frequencies when contrasted with the individual monomers. Frequency analysis of H-bonds plays a crucial role in characterizing their nature and identifying if they are red-shifted or blue-shifted.[102,103]

In general, H-bond interactions and non-covalent interactions have an impact on the frequencies of the interacting molecules. This is reflected in the bond distances of the interacting entities, indicating elongation or contraction. Bond elongation results in a

redshift in the vibrational frequencies, while a blueshift occurs when the bond contracts. Therefore, the frequency shifts provide valuable information about the nature and strength of these interactions.

In some of the chapters the notation A/B//C/D means that the system was first optimised at C/D level of theory and then reoptimised at A/B level of theory. For instance, in Chapter 3 and 4 B3LYP/ccpVTZ//CCSD/cc-pVDZ has been used where it should be read as the system which was initially optimised at CCSD/cc-pVDZ level of theory was further re-optimized at B3LYP/ccpVTZ level of theory and if further frequencies were calculated they must have been calculated at B3LYP/ccpVTZ.

1.6.3 Natural Bond Orbital (NBO) Calculations

Weinhold et al.[104] developed NBO, a mathematical approach that aids in determining the strength of generated H-bond interactions in molecular systems. The NBO suit transforms delocalized molecular orbitals (DMOs) into localised natural bond orbitals (NBOs). The localization of NBOs in a system can vary, ranging from one center to two centers or even three centers. In the case of diatomic molecules, NBOs are formed through a linear combination of NAOs (Natural atomic orbitals) [which are Localized 1-center orbitals can be characterized as the effective "natural orbitals of atom A" within the molecular environment], resulting in two NBOs: the NBO associated with bonding (also called the donor orbital), an occupied orbital, and the NBO related to antibonding (also referred to as the acceptor orbital), a vacant orbital that can accept electrons from the donor NBO orbitals. The NBO method is widely recognized as among the most efficient tools for predicting the strength of H-bonding/Non-Covalent Interactions and the stabilization energy within a specific donor-acceptor interaction region.[105] In a donor-acceptor interaction, the stabilization energy governs the delocalization of electron density. Therefore, the degree of electron density spread in the donor-acceptor interaction is directly influenced by the strength of the stabilizing energy.

Calculating the stabilization energy ($E^{(2)}$) associated with the delocalization of donor (i) to acceptor (j) orbitals is achieved using the subsequent equation[104]:

$$E^{(2)} = \Delta E_{ij} = q_i (F^2_{ij}/\varepsilon_i - \varepsilon_j) \qquad (40)$$

where q_i denotes the occupancy of the donor orbital, and ε_j and ε_i denote the diagonal elements (orbital energies) associated with the NBO Fock matrix. F(i,j) represents the off-diagonal elements related to the same NBO Fock matrix. The strength of hydrogen bonding is directly influenced by the extent of overlap between the NBOs of the donor and acceptor.[104] As the overlap increases, the stabilization energy also increases, resulting in a stronger hydrogen bonding interaction.

1.6.4 Quantum theory of atoms in molecules (QTAIM)

The Quantum Theory of Atoms in Molecules[106] is widely recognized as one of the most effective methods for understanding atom-atom interactions in both covalent and non-covalent molecular systems, including molecular clusters. This theory relies entirely on the analysis of electron density or charge density within the molecule to investigate the bonding nature within molecules or molecular systems. The electron density is typically determined using the following equation:

$$\rho(r, X) = N \int \psi * (x; X)\psi(x; X) d\tau' \qquad (41)$$

In this context, N symbolizes the number of electrons, x corresponds to the electronic coordinate, X denotes the nuclear coordinate, and $d\tau'$ represents the volume element of the system being considered.

The strength of chemical bonds is elucidated through the calculation of bond critical points (BCP). As suggested by Koch and Popelier, BCP offers insights into the routes of H-bonds, wherein electron density exists within the range of 0.002-0.040 a.u., and the Laplacian electron density ranges from 0.024-0.139 a.u.[107] In addition, the topological parameters of bond critical points (BCPs) serve as confirmation for the presence of three distinct types of H-bonds. To address this, Rozas and colleagues[108] introduced three criteria grounded in the Laplacian electron density ($\nabla^2\rho$) and the total electron energy density (H) to delineate the attributes of H-bonds. In cases of hydrogen bonds displaying strong and covalent characteristics, the criteria are $\nabla^2\rho < 0$ and $H < 0$. For hydrogen bonds of moderate and partly covalent attributes, the criteria are $\nabla^2\rho > 0$ and $H < 0$. Lastly, for

hydrogen bonds exhibiting weak and electrostatic features, the criteria are $\nabla^2\rho > 0$ and H > 0. Additional relationships between Laplacian electron density and energetic topological parameters at the bond critical points (BCPs) have been found. One significant relationship involving Laplacian electron density is expressed through the Virial theorem:

$$\frac{1}{4}\left(\nabla^2\rho(r_{BCP})\right) = 2G\left(r_{BCP)}\right) + V\left(r_{BCP)}\right) = H(r_{BCP)} \qquad (42)$$

Here, $G\left(r_{BCP)}\right)$ represents the kinetic energy (positive), $V\left(r_{BCP)}\right)$ represents the potential energy (negative quantity) and $H(r_{BCP)})$ represents the total electron energy densities respectively. By utilizing the kinetic and potential electron density, a comprehensive understanding of the interaction's nature can be achieved. If $V\left(r_{BCP)}\right)$ exceeds $G\left(r_{BCP)}\right)$, the interaction exhibits covalent behavior. On the other hand, if the interaction does not adhere to this relation, it indicates non-covalent behavior. Furthermore, if the kinetic and potential electron density's ratio, exceeds 1, it implies the non-covalent nature of an interaction.[109,110]

1.6.5 Non-Covalent Interaction (NCI) Plot

The non-covalent interaction plot is considered the most effective method for identifying the existence of weaker interactions, whether they occur within a single molecule or between two distinct molecules. It provides valuable insights into the nature and spatial arrangement of these interactions. Bader's theory, known as the Quantum Theory of Atoms in Molecules, along with the NCI index, provides a comprehensive description of weaker interactions.[111] This framework enables a detailed understanding of the nature and characteristics of these NCIs. This approach represents an advanced iteration of the Atom in Molecules theory, offering an enhanced capability for the simultaneous analysis and visualization of diverse NCI types.[112] These interactions are depicted as iso-surfaces of the reduced density gradient in real space, employing the following equation:

$$RDG = \frac{1}{2(3\pi^2)^{1/3}}\frac{|\nabla\rho(r)|}{\rho(r)^{4/3}} \qquad (43)$$

In the equation, ρ(r) denotes the total electron density, while RDG(r) represents the reduced density gradient attributed to the exchange contribution. As per Bader's Atoms in Molecule Theory [113], the expressions for the total electron density ρ(r) and relative to the second highest eigenvalue λ2 of the electron density's Hessian matrix are as follows:

$$\Omega\,(r) = \text{Sign}\,(\lambda 2(r))\,\rho(r) \qquad (44)$$

Where the presence of weak interactions is influenced by both the electron density and the eigenvalue λ2. The sign of λ2 serves to differentiate between bonded attractive interactions (λ2 < 0) and non-bonded repulsive interactions (λ2 > 0). Additionally, the sign of λ2 is utilized to visualize a broad range of interaction types by plotting the reduced density gradient (RDG) against the electron density ρ(r), raised to the power of the sign of λ2. Thus, NCI plots are specifically utilized to visualize the regions where NCIs occur. These plots highlight areas where the reduced density gradient (RDG) approaches zero, indicating regions with low electron density.[111,114] This approach effectively identifies and illustrates the presence of NCIs within a molecular system.

1.6.6 Frontier molecular orbital (FMO) Analysis

The frontier molecular orbital emerges from the fusion of two orbitals: the highest occupied molecular orbital (HOMO) and the lowest unoccupied molecular orbital (LUMO). As per Koopmans' theorem, the ionization energy (I) and electron affinity (A) are connected to the HOMO and LUMO's energies, respectively.[115] In terms of qualitative assessments, the HOMO and LUMO play a significant role in understanding the chemical reactivity and kinetic stability of the system. In addition to facilitating the understanding, these concepts also aid in rationalizing physical and physicochemical properties through the calculation of global descriptors. These descriptors include the electrophilicity index, global softness, electronic chemical potential, global hardness, electronegativity, and maximum charge transfer capability index (ΔNmax). Such calculations contribute to a comprehensive analysis of the system's characteristics and behavior.

Electronic chemical potential $(\mu) = \frac{E_{HOMO}+E_{LUMO}}{2}$ (45)

Global hardness $(\eta) = \frac{E_{LUMO}-E_{HOMO}}{2}$ (46)

Electrophilicity $(\omega) = \frac{\mu^2}{2\eta}$ (47)

Global softness $(S) = \frac{1}{\eta}$ (48)

Electronegativity $(\chi) = -\mu$ (49)

Maximum charge transfer capability index $(\Delta N_{Max}) = \frac{I+A}{2(I-A)}$ (50)

After deriving energy parameters from frontier molecular orbitals (FMOs), significant insights are gained into the chemical reactivity, kinetic stability, and diverse physicochemical properties of the system. Typically, a diminished HOMO-LUMO gap value corresponds to decreased stability and heightened reactivity.

1.6.7 Charge Analysis

1.6.7.1 Hirshfeld Charge

According to Hirshfeld,[116] to offer a numerical portrayal of the distribution of molecular charges, it proves beneficial to partition the molecule into distinctly outlined atomic components. A frequently employed and easily understandable method involves distributing the charge density at each point among the different atoms, mirroring their individual densities as free atoms at the specific distances from the nuclei. This method produces bonded-atom distributions that are well-localized, with each atom closely resembling the molecular density in its immediate vicinity. As reported by Hirshfeld, the total electronic charge in bonded atom is given by:

$$Q_i = -\int \rho_i^{b.a.}(r)\, dv, \quad (51)$$

The negative sign is due to the convention of electrons carrying a negative charge. By incorporating the nuclear charge Z_i, the resulting sum represents the net atomic charge

$$q_i = Q_i + Z_i \quad (52)$$

In practice, the integrand $\rho_i^{b.a.}$ fluctuates too sharply for straightforward numerical integration; hence, integrating the atomic deformation density, is often more convenient, which yields directly the net atomic charge

$$q_i = -\int \delta\rho_i (r)\, dv. \qquad (53)$$

While the calculation of Hirshfeld charges involves integration in real space, the smooth nature of the integrand allows for the direct utilization of advanced grid-based integration schemes within DFT. As a result, the determination of Hirshfeld populations is highly efficient.

1.6.7.2 Merz Kollman (MK) ESP charge and ESP (Electrostatic potential) surface plot

Another extensively acknowledged charge model is the Merz-Kollmann (MK) charge, obtained through the fitting of the electrostatic potential (ESP). In the Merz-Kollmann (MK) method,[117] the fitting points are distributed evenly across layers corresponding to 1.4, 1.6, 1.8, and 2.0 times to each atom's van der Waals radii. However, if the distance between a fitting point and any atom is less than 1.4 times its van der Waals radius, that particular fitting point is disregarded and not included in the fitting procedure.

Electrostatic potential maps provide a three-dimensional representation of charge distribution within a molecular system. They enable the visualization of regions in the molecule with varying charges. By understanding the charge distribution, one can predict the chemical behavior of the molecule and gain insights into its chemical behavior. As per Politzer, the molecular electrostatic potential charge distribution serves as an indicator of the strength of charges, nuclei, and electrons at a particular position within the molecule. The energy needed to move a positive charge from infinity to a given point, V(r), is referred to as the electrostatic potential at that point. Multipole expansion parameters which represent the nucleus and the electron density distribution are both included in each pseudo atom in the improved model, so it is possible to determine the electrostatic potential by evaluating:

$$V(r) = \sum_A \frac{Z_A}{|R_A - r|} - \int \frac{\rho(r')dr'}{|r' - r|} \qquad (54)$$

In the given expression, Z_A represents the charge carried by nucleus A, which is positioned at a distance R_A.[118] By utilizing the electrostatic potential (ESP) charges, potential sites for electrophilic and nucleophilic interactions can be identified.

1.7 Objective of Thesis

The thesis aims to achieve the following objectives to gain comprehensive understanding of the number of conformers, identification of global and local minima conformers, and the stability of these conformers within the molecular system. It does so by investigating both intermolecular and intramolecular hydrogen bonding. Furthermore, we aim to gain insights into metal-molecule interactions by substantiating experimental results through simulated Surface-Enhanced Raman Scattering (SERS).

1. Identifying all potential conformers, including the most stable conformer, for psychedelic molecules such as psilocybin, psilocin, and mescaline. Additionally, the study aims to determine the structural parameters that contribute to their stability.

2. Conformational analysis of molecules that contain both OH and SH groups in their structure, specifically dithiothreitol and thioglycolic acid and exploring the sulfur-centered hydrogen bonding present in the intramolecular and intermolecular systems of these molecules.

3. Investigating molecule-metal interactions using DFT calculations applying molecule-metal modeling approach. It aims to validate the experimental findings regarding the cleavage of cystine on copper and the adsorption behavior of PATP on different metal surfaces.

1.8 References

(1) Eliel, E. L.; Wilen, S. H. *Stereochemistry of Organic Compounds*; John Wiley & Sons, 1994.

(2) Tormena, C. F. Conformational Analysis of Small Molecules: NMR and Quantum Mechanics Calculations. *Prog. Nucl. Magn. Reson. Spectrosc.* **2016**, *96*, 73–88.

(3) *The Nobel Prize in Chemistry 1969*. NobelPrize.org. https://www.nobelprize.org/prizes/chemistry/1969/summary/ (accessed 2023-07-15).

(4) Barton, D. The Conformation of the Steroid Nucleus. 1950. *Experientia* **1994**, *50* (4), 390–394.

(5) Hassel, O.; Viervoll, H.; Sillén, L. G.; Linnasalmi, A.; Laukkanen, P. Electron Diffraction Investigations of Molecular Structures. II. Results Obtained by the Rotating Sector Method. *Acta Chem. Scand.* **1947**, *1*, 149–168.

(6) Hassel, O.; Ottar, B.; Roald, B.; Linnasalmi, A.; Laukkanen, P. The Structure of Molecules Containing Cyclohexane or Pyranose Rings. *Acta Chem Scand* **1947**, *1*, 929–943.

(7) Mazzanti, A.; Casarini, D. Recent Trends in Conformational Analysis. *Wiley Interdiscip. Rev. Comput. Mol. Sci.* **2012**, *2* (4), 613–641.

(8) Vogiatzis, K. D.; Polynski, M. V.; Kirkland, J. K.; Townsend, J.; Hashemi, A.; Liu, C.; Pidko, E. A. Computational Approach to Molecular Catalysis by 3d Transition Metals: Challenges and Opportunities. *Chem. Rev.* **2018**, *119* (4), 2453–2523.

(9) Dell'Angelo, D. Computational Chemistry and the Study and Design of Catalysts. In *Green Chemistry and Computational Chemistry*; Elsevier, 2022; pp 299–332.

(10) Nova, A.; Maseras, F. Enantioselective Synthesis. In *Comprehensive Inorganic Chemistry II (Second Edition): From Elements to Applications*; 2013; pp 807–831.

(11) Melnyk, N.; Iribarren, I.; Mates-Torres, E.; Trujillo, C. Theoretical Perspectives in Organocatalysis. *Chem. Eur. J.* **2022**, *28* (58), e202201570.

(12) Donon, J.; Habka, S.; Mons, M.; Brenner, V.; Gloaguen, E. Conformational Analysis by UV Spectroscopy: The Decisive Contribution of Environment-Induced Electronic Stark Effects. *Chem. Sci.* **2021**, *12* (8), 2803–2815.

(13) Zhang, J.; Zhang, H.; Liu, J.; Lam, J. W. Y.; Tang, B. Z. Visualizing Changes of Molecular Conformation in the Solid-State by a Common Structural Determination Technique: Single Crystal X-Ray Diffraction. *Mater. Chem. Front.* **2021**, *5* (1), 341–346.

(14) Kazerouni, M. R.; Hedberg, L.; Hedberg, K. Conformational Analysis. 21. Ethane-1, 2-Diol. An Electron-Diffraction Investigation, Augmented by Rotational Constants and Ab Initio Calculations, of the Molecular Structure, Conformational Composition, SQM Vibrational Force Field, and Anti-Gauche Energy Difference with Implications for Internal Hydrogen Bonding. *J. Am. Chem. Soc.* **1997**, *119* (35), 8324–8331.

(15) Roque, A. C. A. H.; de Carvalho Santos, D.; Reginato, M. M.; Reis, A. K. C. A. Conformational Analysis for Infrared Spectroscopy and Theoretical Calculations of Some 2-Bromo-2-Propyl 2-Aryl-Acetates, Ibuprofen and Naproxen Analogs. *J. Mol. Struct.* **2021**, *1233*, 130027.

(16) SenGupta, S.; Maiti, N.; Chadha, R.; Kapoor, S. Conformational Analysis of Morpholine Studied Using Raman Spectroscopy and Density Functional Theoretical Calculations. *Chem. Phys. Lett.* **2015**, *639*, 1–6.

(17) Attig, T.; Kannengießer, R.; Kleiner, I.; Stahl, W. Conformational Analysis of N-Pentyl Acetate Using Microwave Spectroscopy. *J. Mol. Spectrosc.* **2013**, *290*, 24–30.

(18) Kobayashi, T.; Arai, T.; Sakuragi, H.; Tokumaru, K.; Utsunomiya, C. A New Method for Conformational Analysis by Photoelectron Spectroscopy with Application to Alkyl-Substituted Styrenes. *Bull. Chem. Soc. Jpn.* **1981**, *54* (6), 1658–1661.

(19) Seeman, J. I.; Secor, H. V.; Breen, P.; Grassian, V.; Bernstein, E. A Study of Nonrigid Aromatic Molecules. Observation and Spectroscopic Analysis of the

Stable Conformations of Various Alkylbenzenes by Supersonic Molecular Jet Laser Spectroscopy. *J. Am. Chem. Soc.* **1989**, *111* (9), 3140–3150.

(20) ALLINGER, N. L.; ALLINGER, J.; GELLER, L. E.; DJERASSI, C. Conformational Analysis. VI. 1a Optical Rotatory Dispersion Studies. XXVII. 1b Quantitative Studies of an α-Haloketone by the Rotatory Dispersion Method. *J. Org. Chem.* **1960**, *25* (1), 6–12.

(21) Rosini, C.; Spada, G. P.; Proni, G.; Masiero, S.; Scamuzzi, S. Conformational Analysis of Some Trans-4, 5-Diaryl-1, 3-Dioxolanes by CD Spectroscopy and Induction of Cholesteric Mesophases in Nematic Solvents: A Correlation between Twisting Power and Structure of the Dopant. *J. Am. Chem. Soc.* **1997**, *119* (3), 506–512.

(22) Kepceoğlu, A.; Köklü, N.; Gündoğdu, Y.; Dereli, Ö.; Kilic, H. Analysis of the Xylenol Isomers by Femtosecond Laser Time of Flight Mass Spectrometry. *Can. J. Phys.* **2018**, *96* (7), 711–715.

(23) Nugent-Glandorf, L.; Scheer, M.; Samuels, D. A.; Bierbaum, V.; Leone, S. R. A Laser-Based Instrument for the Study of Ultrafast Chemical Dynamics by Soft x-Ray-Probe Photoelectron Spectroscopy. *Rev. Sci. Instrum.* **2002**, *73* (4), 1875–1886.

(24) Brady, J. J. *Vaporization of Biological Macromolecules Using Intense, Ultrafast Lasers: Mechanism and Application to Protein Conformation*; Temple University, 2011.

(25) Brady, J. J.; Judge, E. J.; Levis, R. J. Nonresonant Femtosecond Laser Vaporization of Aqueous Protein Preserves Folded Structure. *Proc. Natl. Acad. Sci.* **2011**, *108* (30), 12217–12222.

(26) Bruni, A. T.; Leite, V. B.; Ferreira, M. M. Conformational Analysis: A New Approach by Means of Chemometrics. *J. Comput. Chem.* **2002**, *23* (2), 222–236.

(27) Prize, N. The Nobel Prize in Chemistry 1998. *URL Httpnobelprize Orgnobelprizeschemistrylaureates1999online March 2012* **2019**.

(28) Desiraju, G. R.; Steiner, T. *The Weak Hydrogen Bond: In Structural Chemistry and Biology*; International Union of Crystal, 2001; Vol. 9.

(29) Müller-Dethlefs, K.; Hobza, P. Noncovalent Interactions: A Challenge for Experiment and Theory. *Chem. Rev.* **2000**, *100* (1), 143–168.

(30) Hobza, P.; Rezac, J. Introduction: Noncovalent Interactions. *Chem. Rev.* **2016**, *116* (9), 4911–4912.

(31) Al-Hamdani, Y. S.; Tkatchenko, A. Understanding Non-Covalent Interactions in Larger Molecular Complexes from First Principles. *J. Chem. Phys.* **2019**, *150* (1).

(32) Alkorta, I.; Elguero, J.; Frontera, A. Not Only Hydrogen Bonds: Other Noncovalent Interactions. *Crystals* **2020**, *10* (3), 180.

(33) Kollman, P. A. Noncovalent Interactions. *Acc. Chem. Res.* **1977**, *10* (10), 365–371.

(34) Černỳ, J.; Hobza, P. Non-Covalent Interactions in Biomacromolecules. *Phys. Chem. Chem. Phys.* **2007**, *9* (39), 5291–5303.

(35) Juanes, M.; Saragi, R. T.; Caminati, W.; Lesarri, A. The Hydrogen Bond and beyond: Perspectives for Rotational Investigations of Non-Covalent Interactions. *Chem. Eur. J.* **2019**, *25* (49), 11402–11411.

(36) Latimer, W. M.; Rodebush, W. H. Polarity and Ionization from the Standpoint of the Lewis Theory of Valence. *J. Am. Chem. Soc.* **1920**, *42* (7), 1419–1433.

(37) Burrows, J. A. Pauling, Linus. The Nature of the Chemical Bond and the Structure of Molecules Aid Crystals. Ithaca: The Cornell University Press, 1939. 430 p. $4.50. *Sci. Educ.* **1941**, *25* (2), 120.

(38) Pauling, L.; Corey, R. B.; Branson, H. R. The Structure of Proteins: Two Hydrogen-Bonded Helical Configurations of the Polypeptide Chain. *Proc. Natl. Acad. Sci.* **1951**, *37* (4), 205–211.

(39) Pimentel, G.; McClellan, A. The Hydrogen Bond WH Freeman and Co. *San Franc. Lond.* **1960**, *6*.

(40) Arunan, E.; Desiraju, G. R.; Klein, R. A.; Sadlej, J.; Scheiner, S.; Alkorta, I.; Clary, D. C.; Crabtree, R. H.; Dannenberg, J. J.; Hobza, P.; others. Definition of the

Hydrogen Bond (IUPAC Recommendations 2011). *Pure Appl. Chem.* **2011**, *83* (8), 1637–1641.

(41) Pattabiraman, V. R.; Bode, J. W. Rethinking Amide Bond Synthesis. *Nature* **2011**, *480* (7378), 471–479.

(42) Alkorta, I.; Rozas, I.; Elguero, J. Non-Conventional Hydrogen Bonds. *Chem. Soc. Rev.* **1998**, *27* (2), 163–170.

(43) Grabowski, S. J. Ab Initio Calculations on Conventional and Unconventional Hydrogen Bonds Study of the Hydrogen Bond Strength. *J. Phys. Chem. A* **2001**, *105* (47), 10739–10746.

(44) Biswal, H. S.; Chakraborty, S.; Wategaonkar, S. Experimental Evidence of O–H—S Hydrogen Bonding in Supersonic Jet. *J. Chem. Phys.* **2008**, *129* (18).

(45) Biswal, H. S.; Bhattacharyya, S.; Bhattacherjee, A.; Wategaonkar, S. Nature and Strength of Sulfur-Centred Hydrogen Bonds: Laser Spectroscopic Investigations in the Gas Phase and Quantum-Chemical Calculations. *Int. Rev. Phys. Chem.* **2015**, *34* (1), 99–160.

(46) Gordy, W.; Stanford, S. C. Spectroscopic Evidence for Hydrogen Bonds: SH, NH and NH2 Compounds. *J. Am. Chem. Soc.* **1940**, *62* (3), 497–505.

(47) Stefels, J.; Steinke, M.; Turner, S.; Malin, G.; Belviso, S. Environmental Constraints on the Production and Removal of the Climatically Active Gas Dimethylsulphide (DMS) and Implications for Ecosystem Modelling. *Biogeochemistry* **2007**, *83*, 245–275.

(48) Bates, T.; Lamb, B.; Guenther, A.; Dignon, J.; Stoiber, R. Sulfur Emissions to the Atmosphere from Natural Sourees. *J. Atmospheric Chem.* **1992**, *14*, 315–337.

(49) Beyer, L.; Hoyer, E.; Liebscher, J.; Hartmann, H. Formation of Complexes with N-Acyl-Thioureas. *Z. Chem.* **1981**, *21* (3), 81–91.

(50) Biswal, H. S.; Wategaonkar, S. Sulfur, Not Too Far behind O, N, and C: SH$\cdots\pi$ Hydrogen Bond. *J. Phys. Chem. A* **2009**, *113* (46), 12774–12782.

(51) Karas, L. J.; Wu, C.-H.; Das, R.; Wu, J. I.-C. Hydrogen Bond Design Principles. *Wiley Interdiscip. Rev. Comput. Mol. Sci.* **2020**, *10* (6), e1477.

(52) Wang, J.; Spada, L.; Chen, J.; Gao, S.; Alessandrini, S.; Feng, G.; Puzzarini, C.; Gou, Q.; Grabow, J.-U.; Barone, V. The Unexplored World of Cycloalkene–Water Complexes: Primary and Assisting Interactions Unraveled by Experimental and Computational Spectroscopy. *Angew. Chem.* **2019**, *131* (39), 14073–14079.

(53) Li, S.; Cooper, V. R.; Thonhauser, T.; Puzder, A.; Langreth, D. C. A Density Functional Theory Study of the Benzene- Water Complex. *J. Phys. Chem. A* **2008**, *112* (38), 9031–9036.

(54) Melius, C. F.; Upton, T. H.; Goddard III, W. A. Electronic Properties of Metal Clusters (Ni13 to Ni87) and Implications for Chemisorption. *Solid State Commun.* **1978**, *28* (7), 501–504.

(55) Upton, T. H.; Goddard III, W. A. Chemisorption of Atomic Hydrogen on Large-Nickel-Cluster Surfaces. *Phys. Rev. Lett.* **1979**, *42* (7), 472.

(56) Bauschlicher, C.; Bagus, P. S.; Schaefer, H. Model Study in Chemisorption: Molecular Orbital Cluster Theory for Atomic Hydrogen on Be (0001). *IBM J. Res. Dev.* **1978**, *22* (3), 213–234.

(57) Phala, N. S.; Klatt, G.; van Steen, E. A DFT Study of Hydrogen and Carbon Monoxide Chemisorption onto Small Gold Clusters. *Chem. Phys. Lett.* **2004**, *395* (1–3), 33–37.

(58) Okumura, M.; Kitagawa, Y.; Haruta, M.; Yamaguchi, K. The Interaction of Neutral and Charged Au Clusters with O2, CO and H2. *Appl. Catal. Gen.* **2005**, *291* (1–2), 37–44.

(59) Wu, X.; Senapati, L.; Nayak, S.; Selloni, A.; Hajaligol, M. A Density Functional Study of Carbon Monoxide Adsorption on Small Cationic, Neutral, and Anionic Gold Clusters. *J. Chem. Phys.* **2002**, *117* (8), 4010–4015.

(60) Kadossov, E.; Justin, J.; Lu, M.; Rosenmann, D.; Ocola, L.; Cabrini, S.; Burghaus, U. Gas–Surface Interactions with Nanocatalysts: Particle Size Effects in the Adsorption Dynamics of CO on Supported Gold Clusters. *Chem. Phys. Lett.* **2009**, *483* (4–6), 250–253.

(61) Ding, X.; Yang, J.; Hou, J.; Zhu, Q. Theoretical Study of Molecular Nitrogen Adsorption on Au Clusters. *J. Mol. Struct. THEOCHEM* **2005**, *755* (1–3), 9–17.

(62) Foresman, J. Frisch E.(1993). Exploring Chemistry with Electronic Structure Methods, Gaussian. *Inc Pittsburgh*.

(63) Wu, D.; Hayashi, M.; Shiu, Y.; Liang, K.; Chang, C.; Yeh, Y.; Lin, S. A Quantum Chemical Study of Bonding Interaction, Vibrational Frequencies, Force Constants, and Vibrational Coupling of Pyridine- M n (M= Cu, Ag, Au; N= 2- 4). *J. Phys. Chem. A* **2003**, *107* (45), 9658–9667.

(64) Muniz-Miranda, M.; Muniz-Miranda, F.; Caporali, S. SERS and DFT Study of Copper Surfaces Coated with Corrosion Inhibitor. *Beilstein J. Nanotechnol.* **2014**, *5* (1), 2489–2497.

(65) Ferral, A.; Paredes-Olivera, P.; Macagno, V.; Patrito, E. Chemisorption and Physisorption of Alkanethiols on Cu (111). A Quantum Mechanical Investigation. *Surf. Sci.* **2003**, *525* (1–3), 85–99.

(66) Hieu, T. D.; Chinh, N. T.; Nhung, N. T. A.; Quang, D. T.; Quang, D. D. SERS Chemical Enhancement by Copper-Nanostructures: Theoretical Study of Thiram Pesticide Adsorbed on Cu20 Cluster. *Vietnam J. Chem.* **2021**, *59* (2), 159–166.

(67) Ahmed, A. A. Structural and Electronic Properties of the Adsorption of Nitric Oxide Molecule on Copper Clusters CuN (N= 1–7): A DFT Study. *Chem. Phys. Lett.* **2020**, *753*, 137543.

(68) Crispin, X.; Bureau, C.; Geskin, V.; Lazzaroni, R.; Brédas, J.-L. Local Density Functional Study of Copper Clusters: A Comparison between Real Clusters, Model Surface Clusters, and the Actual Metal Surface. *Eur. J. Inorg. Chem.* **1999**, *1999* (2), 349–360.

(69) Jensen, F. *Introduction to Computational Chemistry*; John wiley & sons, 2017.

(70) Born, M.; Oppenheimer, R. Zur Quantentheorie Der Molekeln Ii Ann, 1927.

(71) Thomas, L. H. The Calculation of Atomic Fields. In *Mathematical proceedings of the Cambridge philosophical society*; Cambridge University Press, 1927; Vol. 23, pp 542–548.

(72) Fermi, E. Un Metodo Statistico per La Determinazione Di Alcune Priorieta Dell'atome. *Rend Accad Naz Lincei* **1927**, *6* (602–607), 32.

(73) Dirac, P. A. M. The Quantum Theory of the Electron. *Proc. R. Soc. Lond. Ser. Contain. Pap. Math. Phys. Character* **1928**, *117* (778), 610–624.

(74) Dirac, P. A. Note on Exchange Phenomena in the Thomas Atom. In *Mathematical proceedings of the Cambridge philosophical society*; Cambridge University Press, 1930; Vol. 26, pp 376–385.

(75) Gombás, P. *Die Statistische Theorie Des Atoms Und Ihre Anwendungen*; Springer-Verlag, 2013.

(76) Hohenberg, P.; Kohn, W. Inhomogeneous Electron Gas. *Phys. Rev.* **1964**, *136* (3B), B864.

(77) Kohn, W.; Sham, L. J. Self-Consistent Equations Including Exchange and Correlation Effects. *Phys. Rev.* **1965**, *140* (4A), A1133.

(78) Vosko, S. H.; Wilk, L.; Nusair, M. Accurate Spin-Dependent Electron Liquid Correlation Energies for Local Spin Density Calculations: A Critical Analysis. *Can. J. Phys.* **1980**, *58* (8), 1200–1211.

(79) Becke, A. D. Density-Functional Thermochemistry. I. The Effect of the Exchange-Only Gradient Correction. *J. Chem. Phys.* **1992**, *96* (3), 2155–2160.

(80) Lee, C.; Yang, W.; Parr, R. G. Development of the Colle-Salvetti Correlation-Energy Formula into a Functional of the Electron Density. *Phys. Rev. B* **1988**, *37* (2), 785.

(81) Burke, K.; Perdew, J. P.; Wang, Y. Derivation of a Generalized Gradient Approximation: The PW91 Density Functional. In *Electronic Density Functional Theory: recent progress and new directions*; Springer, 1998; pp 81–111.

(82) Becke, A. D. Density-Functional Exchange-Energy Approximation with Correct Asymptotic Behavior. *Phys. Rev. A* **1988**, *38* (6), 3098.

(83) Zhao, Y.; Truhlar, D. G. The M06 Suite of Density Functionals for Main Group Thermochemistry, Thermochemical Kinetics, Noncovalent Interactions, Excited States, and Transition Elements: Two New Functionals and Systematic Testing of

Four M06-Class Functionals and 12 Other Functionals. *Theor. Chem. Acc.* **2008**, *120*, 215–241.

(84) Møller, C.; Plesset, M. S. Note on an Approximation Treatment for Many-Electron Systems. *Phys. Rev.* **1934**, *46* (7), 618.

(85) Slater, J. C. The Theory of Complex Spectra. *Phys. Rev.* **1929**, *34* (10), 1293.

(86) Condon, E. The Theory of Complex Spectra. *Phys. Rev.* **1930**, *36* (7), 1121.

(87) Coester, F. Bound States of a Many-Particle System. *Nucl. Phys.* **1958**, *7*, 421–424.

(88) Čížek, J. On the Correlation Problem in Atomic and Molecular Systems. Calculation of Wavefunction Components in Ursell-Type Expansion Using Quantum-Field Theoretical Methods. *J. Chem. Phys.* **1966**, *45* (11), 4256–4266.

(89) Čížek, J.; Paldus, J. Correlation Problems in Atomic and Molecular Systems III. Rederivation of the Coupled-Pair Many-Electron Theory Using the Traditional Quantum Chemical Methodst. *Int. J. Quantum Chem.* **1971**, *5* (4), 359–379.

(90) Cramer, C. J.; Bickelhaupt, F.; others. Essentials of Computational Chemistry. *Angew. Chem.-Int. Ed. Engl.*- **2003**, *42* (4), 381–381.

(91) Raghavachari, K.; Trucks, G. W.; Pople, J. A.; Head-Gordon, M. A Fifth-Order Perturbation Comparison of Electron Correlation Theories. *Chem. Phys. Lett.* **1989**, *157* (6), 479–483.

(92) Davidson, E. R.; Feller, D. Basis Set Selection for Molecular Calculations. *Chem. Rev.* **1986**, *86* (4), 681–696.

(93) Dunning Jr, T. H. Gaussian Basis Sets for Use in Correlated Molecular Calculations. I. The Atoms Boron through Neon and Hydrogen. *J. Chem. Phys.* **1989**, *90* (2), 1007–1023.

(94) Helgaker, T.; Klopper, W.; Koch, H.; Noga, J. Basis-Set Convergence of Correlated Calculations on Water. *J. Chem. Phys.* **1997**, *106* (23), 9639–9646.

(95) Hobza, P.; Müller-Dethlefs, K. *Non-Covalent Interactions: Theory and Experiment*; Royal Society of Chemistry, 2010; Vol. 2.

(96) Balabin, R. M. Enthalpy Difference between Conformations of Normal Alkanes: Intramolecular Basis Set Superposition Error (BSSE) in the Case of n-Butane and n-Hexane. *J. Chem. Phys.* **2008**, *129* (16).

(97) Boys, S. F.; Bernardi, F. The Calculation of Small Molecular Interactions by the Differences of Separate Total Energies. Some Procedures with Reduced Errors. *Mol. Phys.* **1970**, *19* (4), 553–566.

(98) Frisch, M.; Trucks, G.; Schlegel, H. B.; Scuseria, G.; Robb, M.; Cheeseman, J.; Scalmani, G.; Barone, V.; Petersson, G.; Nakatsuji, H.; others. Gaussian 16, 2016.

(99) Lu, T.; Chen, F. Multiwfn: A Multifunctional Wavefunction Analyzer. *J. Comput. Chem.* **2012**, *33* (5), 580–592.

(100) Humphrey, W.; Dalke, A.; Schulten, K. VMD: Visual Molecular Dynamics. *J. Mol. Graph.* **1996**, *14* (1), 33–38.

(101) Neese, F.; Wennmohs, F.; Becker, U.; Riplinger, C. The ORCA Quantum Chemistry Program Package. *J. Chem. Phys.* **2020**, *152* (22).

(102) Roohi, H.; Khyrkhah, S. Ion-Pairs Formed in [Mim+][N (CN) 2-] Ionic Liquid: Structures, Binding Energies, NMR SSCCs, Volumetric, Thermodynamic and Topological Properties. *J. Mol. Liq.* **2013**, *177*, 119–128.

(103) Priya, A. M.; Senthilkumar, L.; Kolandaivel, P. Hydrogen-Bonded Complexes of Serotonin with Methanol and Ethanol: A DFT Study. *Struct. Chem.* **2014**, *25*, 139–157.

(104) Glendening, E.; Badenhoop, J.; Reed, A.; Carpenter, J.; Bohmann, J.; Morales, C.; Landis, C.; Weinhold, F. NBO 6.0, 2013.

(105) Tsipis, A. C.; Tsipis, C. A.; Valla, V. Quantum Chemical Study of the Coordination of Glycolic Acid Conformers and Their Conjugate Bases to [Ca (OH2) n] 2+(N= 0–4) Ions. *J. Mol. Struct. THEOCHEM* **2003**, *630* (1–3), 81–100.

(106) Bader, R. F. Atoms in Molecules. *Acc. Chem. Res.* **1985**, *18* (1), 9–15.

(107) Koch, U.; Popelier, P. L. Characterization of CHO Hydrogen Bonds on the Basis of the Charge Density. *J. Phys. Chem.* **1995**, *99* (24), 9747–9754.

(108) Rozas, I.; Alkorta, I.; Elguero, J. Behavior of Ylides Containing N, O, and C Atoms as Hydrogen Bond Acceptors. *J. Am. Chem. Soc.* **2000**, *122* (45), 11154–11161.

(109) Espinosa, E.; Molins, E.; Lecomte, C. Hydrogen Bond Strengths Revealed by Topological Analyses of Experimentally Observed Electron Densities. *Chem. Phys. Lett.* **1998**, *285* (3–4), 170–173.

(110) Matta, C. F.; Boyd, R. J. An Introduction to the Quantum Theory of Atoms in Molecules. *Quantum Theory At. Mol. Solid State DNA Drug Des.* **2007**.

(111) Wu, P.; Chaudret, R.; Hu, X.; Yang, W. Noncovalent Interaction Analysis in Fluctuating Environments. *J. Chem. Theory Comput.* **2013**, *9* (5), 2226–2234.

(112) Johnson, E. R.; Keinan, S.; Mori-Sánchez, P.; Contreras-García, J.; Cohen, A. J.; Yang, W. Revealing Noncovalent Interactions. *J. Am. Chem. Soc.* **2010**, *132* (18), 6498–6506.

(113) Tang, W.; Sanville, E.; Henkelman, G. A Grid-Based Bader Analysis Algorithm without Lattice Bias. *J. Phys. Condens. Matter* **2009**, *21* (8), 084204.

(114) Contreras-García, J.; Johnson, E. R.; Keinan, S.; Chaudret, R.; Piquemal, J.-P.; Beratan, D. N.; Yang, W. NCIPLOT: A Program for Plotting Noncovalent Interaction Regions. *J. Chem. Theory Comput.* **2011**, *7* (3), 625–632.

(115) Fukui, K. Role of Frontier Orbitals in Chemical Reactions. *science* **1982**, *218* (4574), 747–754.

(116) Hirshfeld, F. L. Bonded-Atom Fragments for Describing Molecular Charge Densities. *Theor. Chim. Acta* **1977**, *44*, 129–138.

(117) Besler, B. H.; Merz Jr, K. M.; Kollman, P. A. Atomic Charges Derived from Semiempirical Methods. *J. Comput. Chem.* **1990**, *11* (4), 431–439.

(118) Politzer, P.; Murray, J. S. The Fundamental Nature and Role of the Electrostatic Potential in Atoms and Molecules. *Theor. Chem. Acc.* **2002**, *108*, 134–142.